Validating retargeted and interpolated locomotions by dynamics-based analysis

Nicolas Pronost*
IRISA, University of Rennes 1
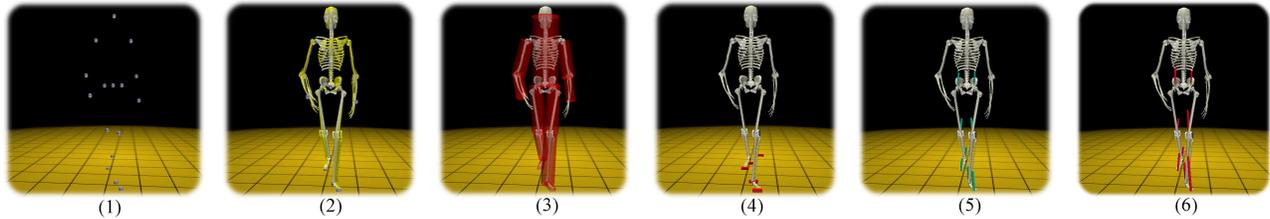
Georges Dumont[†]
IRISA, ENS Cachan

Figure 1: Some steps of our analysis method. From a retargeted and/or interpolated motion (1), our system automatically maps the motion (2) on a mechanical skeleton including masses and inertias information (3). Then we estimate support phases (4), and solve the physical laws, computing resulting forces. We finally validate the motion (5) or not (6) by comparison with literature and experimental data.

Abstract

Retargeting and interpolation methods may introduce physical inaccuracies in virtual human animation. This paper presents a method for evaluating the dynamical correctness of retargeted and interpolated motions. We determine resulting forces and torques at joints, with special attention to the ground reaction forces. With this intention, we propose an automatic creation of the biomechanical model of the character upgraded with the masses and inertias of the limbs and the motion mapping on this model. Then using support phase recognition, we compute resulting forces and torques by an inverse dynamics method.

We evaluate how the retargeting and the interpolation methods change the physics of the motions by using the results of our analysis on artificial and real motions and using literature and experimental data from force plates. Our evaluation relies on the study of several retargeting and interpolation parameters such as the global size of the character, the relative ratios of limbs, the structure of the model, the length of step, the motion style and the character velocity.

CR Categories: I.3.7 [Computer Graphics]: Three-Dimensional Graphics and Realism—Animation

Keywords: Motion analysis, dynamics-based validation, biomechanics

1 Introduction

Synthesising realistic character motion remains one of the great challenges in computer graphics. It seems that obeying physical

*e-mail: npronost@irisa.fr
[†]e-mail: gdumont@irisa.fr

laws is an important criterion of plausibility of motion, which is why the dynamics of human gait have been studied for a long time for animation purposes [Van de Panne et al. 1992; Hodgins 1998; Faure et al. 1997]. The first method to produce such physically realistic motions is to animate characters from captured motion data that are intrinsically valid. These motions are adapted to different representations of the character, to various environments or to additional constraints. The kinematic and kinetic adaptations (by interpolation, edition, retargeting or blending) may introduce physical inaccuracies in virtual human animation. It is thus necessary to be careful when such methods are used, for example using relatively small adaptations [Gleicher and Litwinowicz 1998] or performing modifications within a well-defined class of behaviours [Kovar and Gleicher 2004]. Whenever the modifications introduce visually apparent errors in the physics of motion, dynamics improvements may be added as a post-process or may correct the adaptation algorithm. To this end, Safonova and Hodgins [Safonova and Hodgins 2005] have proposed a method for analysing the correctness of some physical properties in linear interpolated motions.

In this paper, we present a method of dynamics-based validation of retargeting and interpolating algorithms. We study the dynamical correctness of the algorithms through the change in the physics of the adapted motions. This validation relies on the creation of a biomechanical skeleton, i.e a skeleton including information of masses and inertias, and the computation of the resulting forces and torques. Analysing dynamics requires a high number of parameters constraining the motion (including ground support phases) and concerning the subject (including masses and inertias). Our goal is thus twofold: (1) the description of an automatic, generic and stand-alone computation process of the dynamics of a locomotion including the evaluation of these parameters, (2) the application of this process for validating a motion adaptation algorithm with the separation of the influence of the retargeting part and the interpolation part.

The remainder of this paper is structured as follows: section 2 reviews the related works and our contributions, followed by an overview of our method in section 3. The process used for the creation of the biomechanical model of the skeleton is outlined in section 4. Issues concerning dynamics-based analysis are developed in section 5. Finally, validation results are presented in section 6. In section 7, we summarise our contributions, discuss the validation approach and outline possible future research directions.

2 Related works and contributions

Skeleton adaptation and motion interpolation are components of many different approaches for editing [Boulic and Thalmann 1992; Gleicher and Litwinowicz 1998], retargeting [Gleicher 1998; Choi and Ko 2000] or blending [Park et al. 2002; Kovar et al. 2002] human animations. These works aim at producing visually correct motions and do not focus on dynamics correctness. To address this goal, two complementary methods have been proposed: to introduce physical simulation during the adaptation and to correct the motion after the adaptation.

The first method has been the most explored starting with the joint use of space-time constraints on positions and forces [Popović and Witkin 1999]. To reduce the complexity of the optimisations, Fang and Pollard [Fang and Pollard 2003] have proposed a new formulation of the dynamical constraints especially accurate for managing contacts. The optimisation of the forces at the joints involves important computing times. To reduce this complexity, constraints on moment of forces have been added including the mechanical constraints and the motion style [Liu and Popović 2002; Abe et al. 2004]. The zero moment point can then be used to maintain the balance [Tak et al. 2000; Tak and Ko 2005; Zordan and Hodgins 2002]. The method has been extended not to use an iterative process searching optimal solutions at each frame. This method is called dynamics filtering [Yamane and Nakamura 2003]. The authors use a double filtering of the parameters to verify dynamical constraints. The first filtering predicts the next vector state according to kinematical and dynamical constraints such as the respect of the ZMP and the initial posture or the limitation of angular moments. The second filtering corrects the residual inconsistencies between the positions, velocities and accelerations. Another possibility consists in extending the pose control graph of generating models with given postures from motion captures. This method can be used to take into account local contacts and collisions [Zordan and Hodgins 2002; Arikan et al. 2005]. Oshita and Makinouchi [Oshita and Makinouchi 2001] have added masses controlling a subset of the degrees of freedom. In these approaches, the method adds angular moments to those computed by the controllers. These moments can be computed for example as an impulse to return to the initial motion by motion graph [Arikan et al. 2005] or by blending [Zordan et al. 2005] methods.

The second method is more recent, only few works studied physics in interpolated movements. From the idea of determining the kinematic naturalness of a motion [Reitsma and Pollard 2003; Ren et al. 2005], some researchers study the dynamic naturalness. For example, Safonova and Hodgins [Safonova and Hodgins 2005] propose an analysis of the conservation of basic physical properties in interpolated motions such as linear and angular momentum, static balance or friction on the ground. They suggest small modifications to the standard interpolation technique that in some circumstances produce significantly natural looking motions.

In this work, we propose a generic method for validating a method of motion adaptation through the change in the forces and torques at joints. This dynamics analysis is independent of the method of motion adaptation. The resulting forces and torques are compared with biomechanical literature. Moreover we pay special attention to the resulting ground reaction forces, because we can compare them with experimental data from force plates. Our approach relies on a representation of the character including masses and inertias information, that allows to solve the fundamental laws of physics. The process defining this representation is guided by choices and scalings in anthropometrical tables [DeLeva 1996] and linear regression laws [Vaughan et al. 1999]. Our validation algorithm relies on the study of several retargeting and interpolation parameters such as

the global scale of the character, ratios of limbs, the structure of the skeleton, the length of step, the motion style and the character velocity. Thus our contribution can be summarised as follows: the evaluation, for validation purposes, of the resulting forces and torques applied at the joints of the automatically computed biomechanical skeleton.

3 Overview of our system
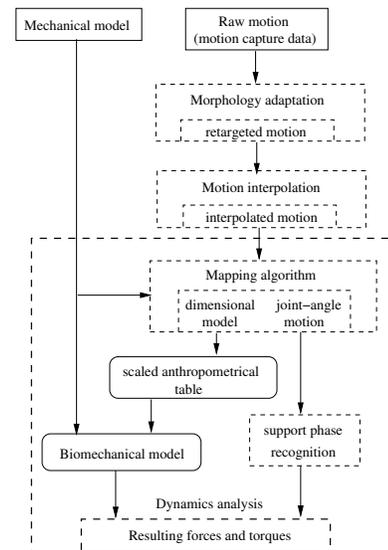
The overview of our system is given in Figure 2.

Figure 2: Analysis system overview. Inputs are a raw (captured) motion and a mechanical chain describing the human skeleton. Outputs are the resulting forces and torques at joints.

In [Pronost et al. 2006], we presented a retargeting algorithm and a motion interpolation process. Now, the questions we want to answer are:

- Are the adapted motions physically valid ?

- If so, what are the limits of the method ?

- And are these limits due to the retargeting or to the interpolation ?

In this paper, we try to answer these questions and illustrate them on our adaptation methods but the analysis is generic and suitable for any method (interpolation, edition, retargeting, blending).

To solve the fundamental laws of physics, and thus analyse the dynamics, we need to evaluate the parameters concerning the subject. The first step is to convert the raw motion data into a joint-angle motion because angular accelerations at joints are needed. We start by defining the articular centers, built from external landmarks. The kinematical chains describing the number of degrees of freedom and the hierarchy of the human skeleton is defined thanks to these landmarks. The motion is then mapped to the human skeleton. The skeleton is thus improved by adjusting the lengths of the limbs. We further attach all the required information such as masses, lengths, circumferences and inertias of limbs, to the model by using anthropometrical tables and regression laws.

To solve the fundamental laws of physics, we also need to evaluate the parameters constraining the motion, i.e. the external forces

acting on the body. So finally, using support phase recognition, we compute resulting forces and torques by an inverse dynamics method.

4 Creation of the biomechanical model

In this section, we present the process that is used to create the biomechanical model of the character. We start by defining the mechanical model describing the hierarchy and the degrees of freedom of the skeleton (in 4.1). Then we need to associate the nodes of this skeleton to articular centers, we define them from the landmarks data (in 4.2). Finally, we upgrade the skeleton with the masses and inertias of the limbs (in 4.3).

4.1 Mechanical model of the skeleton

The Denavit-Hartenberg representation [Hartenberg and Denavit 1955] and its modified notation [Khalil and Kleinfinger 1986] has become a standard for representing robots and for modelling their motions. This representation is a systematic approach to assigning and labelling an orthonormal (x, y, z) coordinate system to each robot joint. It is then possible to relate one joint to the next and ultimately to assemble a complete representation of a robot's geometry. Four parameters are used to define a linear transformation matrix between two successive coordinate systems associated with each joint. These parameters are the length of the link d_j, the distance a_j, the rotation α_j and the angle θ_j between the joints.

The modified representation is adapted within the framework of the representation of a virtual human skeleton. Indeed, the hierarchy of our skeleton is directly incorporated in the representation, as well as the expression of the position and the orientation of a joint in the parent reference frame.

Our system computes, for the whole motion, average values of distances between the articulations. These values define the translation parameters d_j and a_j. We just have to provide the rotational parameters α_j and θ_j.

4.2 Definition of the articular centers

We compute the articular centers for two reasons: to map the motion on an angular-based skeleton and to use the anthropometrical tables describing physical properties from distances between articular centers. Some researchers have focused on problems related to estimation of the joints of a skeleton from magnetic data [O'Brien et al. 2000; Kirk et al. 2005], from optical marker data [Silaghi et al. 1999; Zordan and Van Der Horst 2003] and also for interaction purposes [Oore et al. 2002; Shin et al. 2001].

In our approach, articular centers are not computed from the evolution of the relative positions of limbs but from the landmarks. At each frame, we have to compute the three-dimensional positions $P(a)$ for each articular system a that we want to simulate. We use the set of the three-dimensional positions of the landmarks $P(l)$. We just have to associate at least one $P(l)$ with one $P(a)$. The main interest is that it helps us to define a very accurate position of an articular center (see example below) or a virtual position like the root of the skeleton (using pelvis landmarks, for example). Moreover, it allows us to define articular centers and then a model from any marker set.

Example: the knee. We place 4 motion capture landmarks on the lateral epicondyles and the medial epicondyles of femurs and tibiae. We compute the average value of these four points, and consider it

as the articular center of the knee. The knee articulation is then defined by this point and the rotation axes depending on 3D positions of the neighbouring articular centers.

4.3 Attaching masses and inertias

Physical information that are necessary and sufficient to enable us to solve the problem of inverse dynamics are the masses and inertias of the limbs. Other biomechanical information may be added to take into account additional constraints [Liu et al. 2005], such as muscles activation preferences, elastic mechanism and variable stiffness at joints.

Since anthropometrical tables are different depending on the gender of the character, we provide this information. For the same reason, we have to assign semantics to the skeleton, i.e. associate a segment between two articulation systems to a human limb. The semantics can be given manually or assigned automatically if the articular systems have preset labels.

We model limbs by using cylinders of homogeneous density because most of the anthropometrical tables and laws use this representation. From the evaluation of the lengths of the limbs (a_j parameters), we are able to estimate the total human height H and mass M by using tables described in [DeLeva 1996]. We use linear regression laws [Vaughan et al. 1999] to estimate masses and inertias for each limb l:

- Mass

$$m_l = a.M + b.l_l.c_l^2 + c \qquad (1)$$

  where m_l is the mass of limb l, l_l its length, c_l its circumference and (a, b, c) three coefficients depending on the gender and the limb.

- Inertia

$$I_l = a.M.(b.l_l^2 + c.c_l^2) + d \qquad (2)$$

  where I_l is the inertia of limb l, and (a, b, c, d) four coefficients depending on the gender and the limb.

These equations are well established for lower-limbs. For the upper body, masses are directly assigned by proportional values from scaled tables, and inertias are computed thanks to the radius of gyration:

$$I_l = m_l.(l_l.r_l)^2 \qquad (3)$$

where r_l is the radius of gyration expressed as a percentile of l_l.

5 Dynamics analysis

The inverse dynamics problem was studied for a long time for animation purposes [Ko and Badler 1996]. Because solving dynamics needs angular acceleration data, we compute articular trajectories during the motion. Thus, we project the motion to the skeleton (section 5.1), that is to say, we geometrically reconstruct the postures according to the motion and the biomechanical model.

5.1 Articular trajectories

In this section, we address the mapping issue going from 3D positions of articular centers to the joint-angle posture of the character. In general, mapping a motion to a physical model is an underconstrained problem and optimisation requires additional metrics to find a unique posture, for example with optimised-based IK

approaches [Zhao and Badler 1994] or spatial constraints [Bindi-ganavale and Badler 1998] to preserve end effector positions.

We solve the mapping problem for each articular system (i.e. co-localised Denavit-Hartenberg joints set) in sequence by using direct geometrical reconstruction, i.e. computing the rotation matrix between the current and the next articular center allowing to be the closest possible to the desired position.

- If the articulation is a pin joint, the dot product between the normalised vectors representing the limbs gives the *cosine* of the required angle θ'_j. We add θ'_j to it's initial value defined by the mechanical model.

- If the articulation is a spherical joint, we must choose the rotation matrix among an infinity of solutions. But we often have additional constraints which reduce the number of solutions. For example if the next articulation is a pin joint, we can determine the future error and then choose the rotation matrix minimising it. Average values can also be computed as long as the next articulations are pin joints for minimising the successive errors. If we do not have additional constraints, we compute the minimal rotation compared to the previous reference frame.

5.2 Support phase recognition

To solve the inverse dynamics problem, we need to know external forces that are applied to the system. For locomotion, these forces are: gravity, ground reaction forces and aerodynamic friction forces. The application of gravity is straightforward and we suppose that aerodynamic friction forces are negligible. We focus here on the determination of the ground reaction forces. This determination is performed in two steps. In the first step, we define the ground contacts i.e. the heels strikes and toes off. The second step consists in applying Newton's second law of motion to determine the resulting forces and torques.

We determine the start of the heels contacts and the end of the toes contacts, and then we apply the appropriate inverse dynamics resolution according to the stance phase (see 5.3). Recent works [Ikemoto et al. 2006] show the limits of using *speed* and *height* methods to discriminate foot plants. *speed* and *height* are methods based on thresholds (of speed and vertical amplitude) below which the feet are assume to be in support. They use instead a learning method based on the training of limbs positions in hand-labeled motions. Here, to be rather generic, we studied four recognition methods with four sets of possible support joints. We present in this section the used principles and results of these methods with our previous example of foot support: toes and heels.

Our reference method is a hand-labeled estimation, called *visual*, that will serve to compare the methods described hereafter. We evaluate the *speed* and *height* methods. We add a configuration-based method, called *config*, which uses particular relative joints configurations (toes and heels) at full extension and flexion. These configurations are detected as local maxima for extension and crossing coordinates for flexion. These three methods predict which frames are the start and the end of the ground contact.

We present in Table 1, the evaluations of these recognition methods through the four following criteria.

Number of failures. We assume that the *visual* method never fails. The *speed* and *config* methods never failed with the set of 12 motions, and the *height* method has a 66% rate of returning a valid result.

method/criterion	Nb failures	Error	S.D.	S.D. norm.
speed	0	2.3	1.6	0.50
height	16	5.6	2.4	0.41
config	0	9.7	2.1	-

Table 1: Results (in frames, except for the normalised S.D.) are established in comparison with the *visual* reference method. We evaluate the methods on 12 different locomotions, so on 12×2(left-right)$\times 2$(flexion-extension)= 48 contacts.

The average error is: $\bar{e} = \frac{\sum_{i=1}^{N} |F_{ref_i} - F_{eval_i}|}{N}$, where F_{ref_i} is the reference frame of the contact i (defined by *visual*), F_{eval_i} is the evaluated frame, and N is the number of contacts (48 in our example). This is the mean difference, in frames, of the resulting heels strikes and toes off evaluations. Errors for *speed* and *height* methods are acceptable, but for *config*, a value of 9.7 (i.e. 0.17 s) is quite large.

The standard deviation of the error is: $sd = \sqrt{\frac{\sum_{i=1}^{N} (e_i - \bar{e})^2}{N}}$, where e_i is the error of contact i, and $\bar{e}$ is its average error. This criterion shows the stability of the recognition algorithms. We note again the good accuracy of the speed-based methods, height-based and configuration-based are acceptable.

The normalised standard deviation of thresholds values is: $sdn = \frac{\sum_{i=1}^{p} sd(threshold)}{p.\overline{threshold}}$, where $sd(threshold)$ is the standard deviation of the values of the threshold, $\overline{threshold}$ is their average error, and p is the number of parameters (2 in our two methods *speed* and *height*). This criterion shows the stability of the speed and the amplitude thresholds. We see here the main interest in the *config* method, since we do not need any threshold. None of both others seems really better. But we can note that the thresholds are rather stable, which enables us to integrate average values for any locomotion (see Table 2).

	heel strike	toe off
height (%)	13.0	13.37
speed (m/s)	0.73	0.39

Table 2: Average values of thresholds. Amplitudes are in percentile of the maximum elevation of the foot during the walk cycle.

We performed the same statistical calculations for three other configurations of support points: *ankle and toe*, *heel alone* and *ankle alone*. Results show the importance of the methods using the heel (in extension phase detection) and the toe (in flexion phase detection). Our recognition algorithm uses the most adapted method according to its quality and to the configuration of the skeleton. In our configuration, *heel and toe*, the most adapted method is the *speed* method.

5.3 Resulting forces and torques

In this section, we apply Newton's second law of motion. Thanks to the knowledge of the ground support phases and the biomechanical model of the skeleton, we are able to compute the resulting forces and torques acting at the joints: toes, heels, knees, hips, shoulders, elbows and hands. To accomplish these computations, we provide an inverse dynamics process using only a few key steps.

The structure of Newton's second law of motion depends on the external forces applied to the body. We solve it according to the external forces which are the ground reaction forces. For locomotions, there are three different states: single support, double

support and no support.

Linear form of Newton's second law:

The summation of external forces acting on a limb l is equal to the product of its mass m_l (supposed constant) by the acceleration $\vec{a}$ of its center of gravity G_l:

$$\sum \overrightarrow{Forces}_l = m_l.\vec{a}_{G_l} \tag{4}$$

- single support

During single support phase we recursively solve the linear form of Newton's second law from free effectors (foot not in support and hands) to the support foot. Only the gravity acts on the free limbs as an external force, we can solve the equation for these limbs and calculate the force acting on the next limb, and so on.

- double support

When the character is in double support phase, the previous solving algorithm can not be directly applied because the two ground reaction forces $\overrightarrow{FR_1}$ and $\overrightarrow{FR_2}$ are unknown. But the acceleration of the center of gravity G of the whole system leads to the equation:

$$\overrightarrow{FR_1} + \overrightarrow{FR_2} + (-\vec{g}).\sum m_l = (\sum m_l).\vec{a}_G \tag{5}$$

where $(-\vec{g}).\sum m_l$ is the total weight of the character. To solve this two-unknowns equation, we use the angular expression of Newton's law expressed at point G:

$$\overrightarrow{G\,O_1} \times \overrightarrow{FR_1} + \overrightarrow{G\,O_2} \times \overrightarrow{FR_2} = [I]_G.\vec{\dot{\omega}}_G \tag{6}$$

where O_1 and O_2 are the known positions of support, $[I]_G$ the inertia matrix and $\vec{\dot{\omega}}_G$ the angular acceleration vector. The angular momentum term is equal to zero because there is no localised momentum at these support points. With these two equations we are able to compute the ground reaction forces and then iteratively solve the linear equation from supports to hips.

- no support

During a flying phase, the computation is straightforward, there is no additional force, then we solve for the four chains independently from free segments to the trunk. This case is useful for running movements and jumps. We thus obtain the internal forces for any locomotion style.

Angular form of Newton's second law:

The summation of external torques acting on a limb l is equal to the rate of change of its angular momentum:

$$\sum_j (\overrightarrow{G_l\,O_j} \times \vec{F}_{j/l}) + \sum_j \vec{C}_{j/l} = [I]_{G_l}.\vec{\dot{\omega}}_{G_l} \tag{7}$$

where O_j is the application point at joint j of the external force $\vec{F}_{j/l}$ acting on l, and $\vec{C}_{j/l}$ is the angular momentum at O_j.

We can thus use the following algorithm to solve the angular equation at each articulation `a` associated to a limb `l`.

```
FOR ALL articulation a DO
   weight_l = {0.0, 0.0, -g . m_l}
   Moment_due_to_weight_a = |a_G_l| × weight_l
   Moment_due_to_force_a-1 = |a(a-1)| × force_a-1
   torque_a = [I]_G_l.ω_G_l - Moment_due_to_force_a-1 -
Moment_due_to_weight_a - torque_a-1
   DONE
```

6 Experimental results

We have finally reached our analysis objective that is to compute the resulting joint forces and torques. In this section, we answer the questions presented in section 3, with a special focus on the Ground Reaction Forces (GRF).

6.1 Self-coherent validation

The first question is: are the adapted motions physically valid ? To answer this question, we apply *direct* adaptations, i.e. we apply the retargeting on an known real morphology and we only use real data of this character to interpolate the motion. Figure 3 shows the comparison of the GRF of such *direct* adapted motions with force plates measures of same characters.
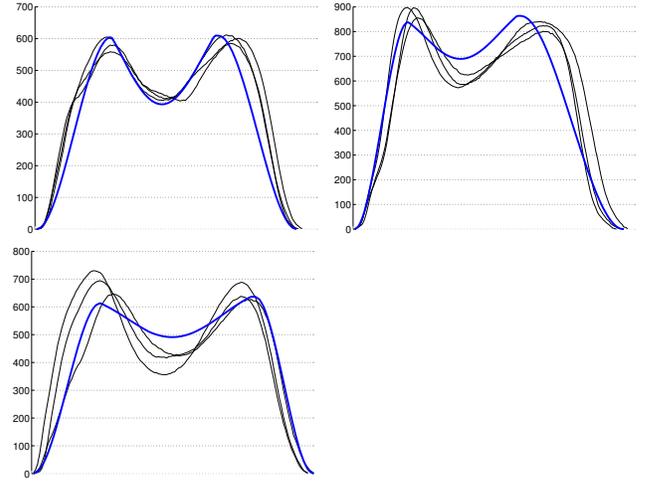

Figure 3: Top left: a 55.4kg man, top right: a 79.6kg man, bottom: a 58.2kg woman. The black plots are 3 ground reaction forces (in Newton) measured by force plates for these characters. The blue plots are analysed ground reaction forces from normal locomotions with the biomechanical data of the same characters.

The experimental measures show that the first character produces an almost constant GRF, related to an immutable style of locomotion. Our *direct* adaptation process does not have difficulties reproducing the same movement and thus the same GRF. In the second experimentation, the style of the capture locomotions is variable, the adapted GRF thus have identical local maxima but different characteristics of the motion (see 6.3). The third experimentation shows irregular captured GRF, the resulting adapted force is different while remaining valid on the maximum amplitudes, results probably due to the shifting of velocity (see 6.3.3).

We analyse different styles of locomotions and pay attention to the GRF (Figure 12 and Figure 4). We compare these analysis results with data described in literature [Vaughan et al. 1999; Faure et al. 1997; Apkarian et al. 1989]. Our dynamics analysis of locomotions gives valid results compared with literature and real measures. We observe a few well-known properties. The range (in Newtons) for the vertical force is almost three times that of the fore-aft force. This vertical force also has the double hump generally observed in biomechanics, and exceeds body weight at two different times during the stance phase. The lateral force has a range of less than one tenth of the vertical force. During most of the stance phase, this force is negative, which means that the ground is pushing inward on

the character's foot. The fore-aft force acts in a backward direction during the first half of the support, and becomes the opposite as the character pushes off. We verify other known biomechanical properties such as support duration and torques values.
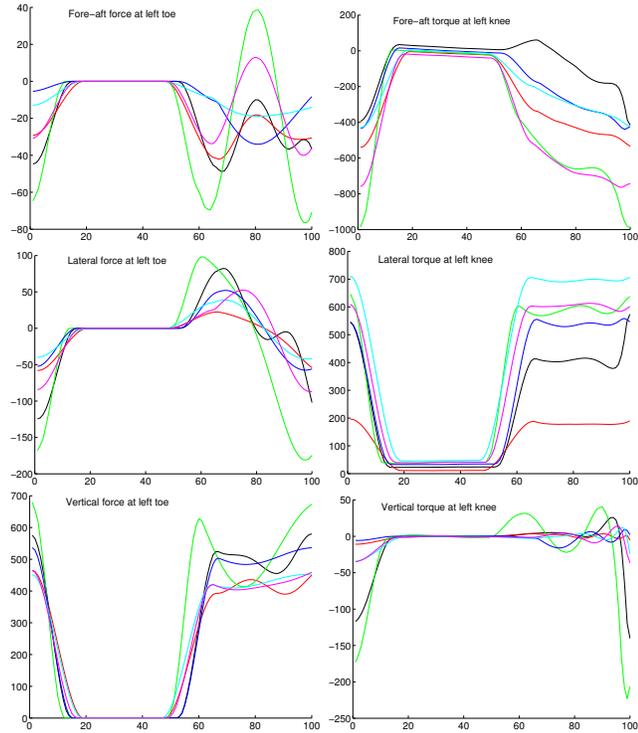

Figure 4: Left: Resulting forces (in N) at left toe for 6 real analysed locomotions. Right: Torques (in N.m) at left knee for the same locomotions. A full gait cycle is plotted from a right heel strike to the next one.

We show here results only on the left GRF and on the torques at left knee, but we made the same validation on forces and torques at all the other joints. We so assume that our process answer positively to our first question concerning the validation. There remains the next two questions: what are the limits of the method, and are these limits due to the retargeting or to the interpolation ? We then study separately their influence on the GRF and we determine their limits.

6.2 Influence of retargeting

In order to study the influence of retargeting on the physical realism of the adapted motion, we observe the resulting forces when we change the morphology of the targeted character. So this study recover how the retargeting algorithm changes the physics of the motion, but has no relation to how the real physics change when the morphology change. For that, we plan to capture locomotions and foot strike force data for real subjects corresponding to the changed physical parameters.

6.2.1 Global scale

We retarget one non-interpolated motion on 8 different morphologies and examine the GRF (Figure 5(a)). All limbs are scaled from half to double size of the initial skeleton. Results shows that the global size of the character has a huge influence on the dynamics,

indeed the masses are the main parameters in equation (4). In order to be able to compare these GRF, we have to normalize them. We looked for the relation between the scale on the morphology and the scale on the GRF minimising the root mean square (RMS) cumulated error (order 1). We show this relation in Figure 5(b), and we observe that this relation is a linear function. We also compare the GRF with experimental data of real characters. We verified this relation by experimental data on several locomotions and subjects between 0.7 and 1.2 scales. Under 0.7 and over 1.2, we suppose that this relation is still valid.
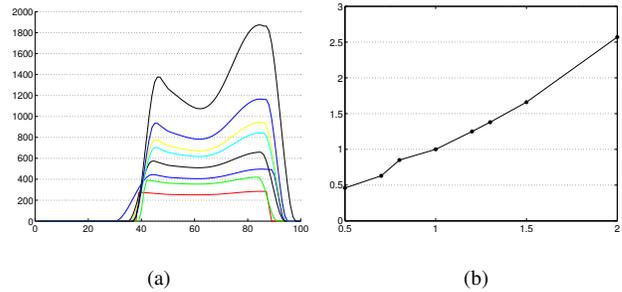

(a) (b)

Figure 5: Influence of a global scale. We retarget one locomotion on 8 morphologies: x0.5, x0.7, x0.8, x1.0, x1.2, x1.3, x1.5 and x2.0. The resulting GRF (in Newtons) are linearly dependant of the scale.

6.2.2 Femur/Tibia ratio

In this section we study the influence of the modification of relative lengths of limbs. This influence is useful to evaluate the initial errors in the articular centers estimations. Here, we change the femur/tibia length ratio without changing the global length of the leg. Resulting GRF are plotted in Figure 6(a). We present in Figure 6(b) the RMS cumulated errors between GRF of the retargeted and the original motions. We can not compare the results with many experimental data, because most of the observed ratios are close. These ratios lie between 0.7 and 1.3, and RMS errors in this range are quite small (approximately 3 Newtons). When we observe the 0.6 ratio error, we can suppose that retargeting a locomotion out of this range probably produces a non valid motion.
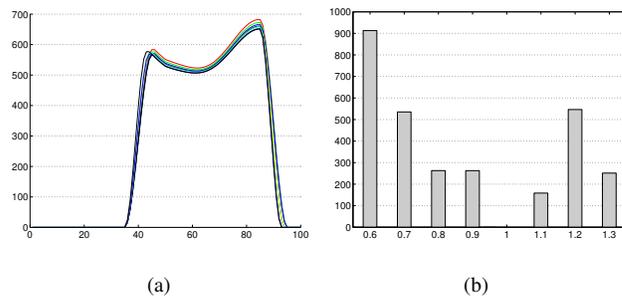

(a) (b)

Figure 6: Influence of the femur/tibia ratio. We retarget one locomotion with 8 ratios: 0.6, 0.7, 0.8, 0.9, 0.95, 1.1, 1.2 and 1.3. Our initial ratio is 0.95.

We can note another logical but important phenomenon of which we must be careful. When a motion is adapted, the movements of the heaviest limbs are the most influent. We can easily observe this phenomenon if we change the upper/lower body ratio (not presented in this paper), because the trunk has much more mass than others limbs.

6.2.3 Structure of the skeleton from degrees of freedom

In this section we change the structure of the skeleton. We retarget one locomotion on two skeletons with 38 and 26 degrees of freedom. They differ by the following articulations: elbows, knees and ankles where the spherical joints (3 dof) become pin joints (1 dof). Figure 7 shows the cumulated 3D distances between the positions of centers of gravity of all the 11 limbs.
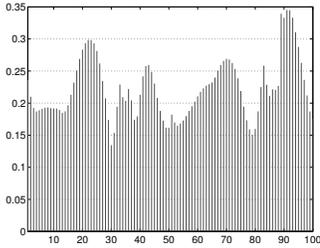
Figure 7: The sum of the Euclidean distances (in meters) of the positions of the centers of gravity of limbs during the cycle between a 38 dof and a 26 dof skeleton.

The average error value is 0.22 meters, so 2 cm per limbs. This value is not small, but is it significant ? The resulting GRF are plotted in Figure 8(a) and we present in Figure 8(b) the RMS errors between the GRF of the two retargeted motions.
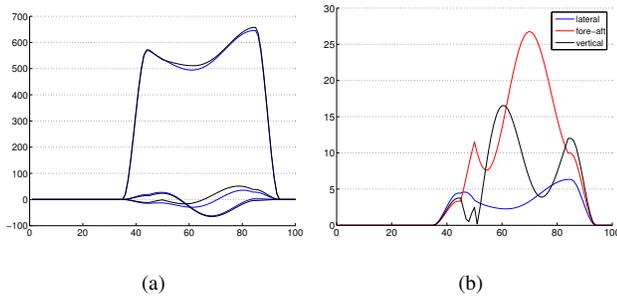
(a)   (b)

Figure 8: Influence of the structure of the skeleton. We plot the 3D GRF (in blue: the 38 dof model, in black: the 26 dof model) and their RMS errors during the locomotion cycle.

The lateral error is very small and this is logical because during locomotion the linear acceleration of limbs on this axis is low. If we retarget a locomotion on a more restrictive skeleton (less dof), the influence on the fore-aft axis is more important than on the vertical axis. Thus when we retarget a motion, we must be careful of the fore-aft acceleration of limbs. In this example, the higher GRF difference is equivalent to a modification of the weight of the character by 2.5 kilogrammes.

6.3 Influence of the interpolation

In order to study the influence of the interpolation on the physical realism of the adapted motion, we observe the GRF when we change locomotor parameters of the motion. We present three of these parameters which can be modified independently.

6.3.1 Length of step

In this section we study the influence of the modification of the length of the step. This influence is useful to evaluate the footskate corrections often used in adaptation methods. These corrections mainly change the articular trajectories by an inverse kinematics method but also the position of the foot, and so the length of the step. We change the initial length of the step l_s, creating 8 new lengths $l = \alpha \times l_s$ with $\alpha = 0.6$ to 1.3. The resulting GRF are plotted in Figure 9(a) and RMS cumulated errors in Figure 9(b).
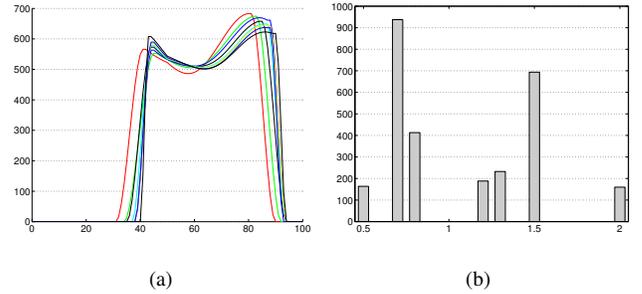
(a)   (b)

Figure 9: Influence of the length of the step. We interpolate the locomotion with eight α values: 0.6, 0.7, 0.8, 0.9, 0.95, 1.1, 1.2 and 1.3.

These figures show that there is no apparent correlation between the lengths of step and the GRF. That can be due to two reasons: (1) the interpolation is correct, the GRF are not linearly correlated with the length of step, or (2) the interpolation is incorrect and we can not know how the GRF evolves. In regard to the interpolation method, the first solution can be valid because the interpolation is not linear, but based on a discrete database of motions. To be sure, we plan to acquire more force plates measures including a large range of step length data.

6.3.2 Motion style from posture

In this section we want to change the motion style. We choose to use the rest posture of the character which is driven by the erect percentile Er of the character. We test 8 erect percentiles $E = \theta \times Er$ with $\theta = 0.8$ to 1.15. The resulting GRF are plotted in Figure 10(a) and RMS cumulated errors in Figure 10(b).
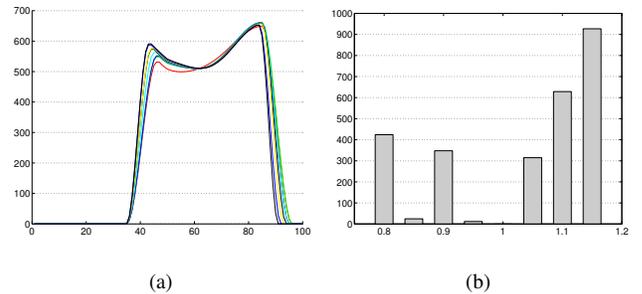
(a)   (b)

Figure 10: Influence of the motion style. We interpolate the locomotion with eight θ values: 0.8, 0.85, 0.9, 0.95, 1.0, 1.05, 1.1 and 1.15.

We observe that if we interpolate the motion on a more bent style, errors are not significant. On the other hand, the interpolation on a very erect style increases the error. We explain this phenomenon assuming that high erect postures prevent doing large steps. If we

force it, the interpolation may introduce GRF errors. We conclude that interpolating to less erect styles of locomotion is safer.

6.3.3 Character velocity

In this section we change the velocity v_i of a walk, creating 8 velocities $v = \gamma \times v_i$ with $\gamma = 0.67$ to 1.33. The resulting GRF are plotted in Figure 11(a) and RMS cumulated errors in Figure 11(b).
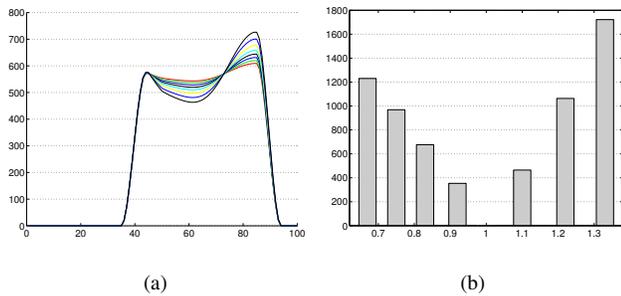

(a)   (b)

Figure 11: Influence of the speed. We interpolate one walk with eight γ values: 0.67, 0.75, 0.83, 0.92, 1.0, 1.1, 1.22 and 1.33.

When we decrease the speed, the error increases but the physical properties are preserved. When the speed increases, the amplitude of the double hump during support phase increases up to invalid values. At this time, the interpolation process must change the motion style to a running locomotion (not managed in our approach).

7 Conclusion

In this paper, we have presented a method of dynamics-based analysis of retargeted and interpolated locomotions with the aim of validating the used adaptation algorithm. In this method, we first define the human model as a biomechanical representation of the character. This representation is created by improving a given mechanical model of the skeleton using anthropometrical tables and regression laws. The second stage consists in defining a transformation process which enables us to work with a joint-angle motion. Finally, using support phase recognition, we check the correctness of the forces and torques with special attention to the ground reaction forces.

This process is automatic, generic and independent of the adaptation method. Here, the process is applied to retargeted and interpolated locomotions, but it can be used on real motions or on edited or blended motions. We have presented this approach as a post-process for dynamics analysis, but the method used could be performed in real-time during the adaptation algorithm. Thus, we plan to implement our algorithm directly in our adaptation method. We also have to try to overcome the standard limitation of inverse dynamics such as the uniform distribution of masses or the joint and air frictions, to improve our inverse dynamics algorithm. Thus, our future work is to orient the analysis and the synthesis of motions through the forces and torques for examples of energetic cost estimation, effort-based interpolations or motion recognition and classification.

References

ABE, Y., LIU, C., AND POPOVIĆ, Z. 2004. Momemtum-based parametrization of dynamic character motion. In *ACM Siggraph / Eurographics Symposium on Computer Animation*, 173–182.

APKARIAN, J., NAUMANN, S., AND CAIMS, B. 1989. A three-dimensional kinematic and dynamic model of lower limb. *Journal of Biomechanics 22*, 143–155.

ARIKAN, O., FORSYTH, D., AND O'BRIEN, J. 2005. Pushing people around. In *ACM Siggraph / Eurographics Symposium on Computer Animation*, 59–67.

BINDIGANAVALE, R., AND BADLER, N. 1998. Motion abstraction and mapping with spatial constraints. *Lecture Notes in Computer Science 1537*, 70–82.

BOULIC, R., AND THALMANN, D. 1992. Combined direct and inverse kinematic control for articulated figure motion editing. *Computer Graphics Forum 11(4)*, 189–202.

CHOI, K., AND KO, H. 2000. On-line motion retargetting. *The Journal of Visualisation and Computer Animation 11(5)* (December), 223–235.

DELEVA, P. 1996. Adjustments to Zatsiorsky-Seluyanov's segment inertia parameters. *Journal of Biomechanics 29 (9)* (September), 1223–1230.

FANG, A., AND POLLARD, N. 2003. Efficient synthesis of physically valid human motion. *ACM Transactions on Graphics 22 (3)* (July), 417–426.

FAURE, F., DEBUNNE, G., CANI, M., AND MULTON, F. 1997. Dynamic analysis of human walking. In *Eurographics Workshop on Computer Animation and Simulation (EGCAS)*.

GLEICHER, M., AND LITWINOWICZ, P. 1998. Constraint-based motion adaptation. *The Journal of Visualization and Computer Animation 9*, 2, 65–94.

GLEICHER, M. 1998. Retargetting motion to new characters. In *SIGGRAPH '98: Proceedings of the 25th annual conference on Computer graphics and interactive techniques*, 33–42.

HARTENBERG, R., AND DENAVIT, J. 1955. A kinematic notation for lower-pair mechanisms based on matrices. *Journal of Applied Mechanics* (June), 215–221.

HODGINS, J. 1998. Animating human motion. *Scientific American 278 (3)* (March), 64–69.

IKEMOTO, L., ARIKAN, O., AND FORSYTH, D. 2006. Knowing when to put your foot down. In *Symposium on Interactive 3D Graphics and Games (I3D)*.

KHALIL, W., AND KLEINFINGER, J. 1986. A new geometric notation for open and closed loop robots. In *ICRA'86*, 75–79.

KIRK, A., O'BRIEN, J., AND FORSYTH, D. 2005. Skeletal parameter estimation from optical motion capture data. *Computer Vision and Pattern Recognition 2005 2* (20-25 June), 782–788.

KO, H., AND BADLER, N. 1996. Animating human locomotion with inverse dynamics. *IEEE Computer Graphics and Applications 16(2)*, 50–5.

KOVAR, L., AND GLEICHER, M. 2004. Automated extraction and parametrization of motions in large data sets. *ACM Transactions on Graphics 23 (3)* (August), 559–568.

KOVAR, L., GLEICHER, M., AND PIGHIN, F. 2002. Motion graphs. In *Proceedings of SIGGRAPH'02*.

LIU, C., AND POPOVIĆ, Z. 2002. Synthesis of complex dynamic character motion from simple animation. *ACM Transactions on Graphics 21 (3)* (July), 408–416.

LIU, C., HERTZMANN, A., AND POPOVIĆ, Z. 2005. Learning physics-based motion style with nonlinear inverse optimization. *ACM Transactions on Graphics 24 (3)* (July), 1071–1081.

O'BRIEN, J., BODENHEIMER, R., BROSTOW, G., AND HODGINS, J. 2000. Automatic joint parameter estimation from magnetic capture data. In *Proceedings of Graphics Interface'00*, 53–60.

OORE, S., TERZOPOULOS, D., AND HINTON, G. 2002. Local physical models for interactive character animation. *Computer Graphics Forum / EG2002 Proceedings 21 (3)*.

OSHITA, M., AND MAKINOUCHI, A. 2001. A dynamic motion control technique for human-like articulated figures. *Computer Graphics Forum / EG2001 Proceedings 20 (3)*, 192–202.

PARK, S., SHIN, H., AND SHIN, S. 2002. On-line locomotion generation based on motion blending. In *ACM Siggraph / Eurographics Symposium on Computer Animation*, 105–111.

POPOVIĆ, Z., AND WITKIN, A. 1999. Physically based motion transformation. In *Proceedings of SIGGRAPH'99*, 11–20.

PRONOST, N., DUMONT, G., BERILLON, G., AND NICOLAS, G. 2006. Morphological and stance interpolations in database for simulating bipedalism of virtual humans. *The Visual Computer 22*, 1 (January), 4–13.

REITSMA, P., AND POLLARD, N. 2003. Perceptual metrics for character animation: Sensitivity to errors in ballistic motion. *ACM Transactions on Graphics - SIGGRAPH 2003 Proceedings 22(3)*, 537–542.

REN, L., PATRICK, A., EFROS, A., HODGINS, J., AND REHG, J. 2005. A data-driven approach to quantifying natural human motion. *ACM Transactions on Graphics (SIGGRAPH 2005) 24(3)*, 1090–1097.

SAFONOVA, A., AND HODGINS, J. 2005. Analyzing the physical correctness of interpolated human motion. In *ACM Siggraph / Eurographics Symposium on Computer Animation*, 171–180.

SHIN, H., LEE, J., GLEICHER, M., AND SHIN, S. 2001. Computer puppetry: An importance-based approach. *ACM Transactions of Graphic 20(2)*, 67–94.

SILAGHI, M., PLANKERS, R., BOULIC, R., FUA, P., AND THALMANN, D. 1999. Local and global skeleton fitting techniques for optical motion capture. *CAPTECH'98: Modeling and Motion Capture for Virtual Environments 1537* (November), 26–40.

TAK, S., AND KO, H. 2005. A physically-based motion retargeting filter. *ACM Transaction on Graphics 24(1)*, 98–117.

TAK, S., SONG, O., AND KO, H. 2000. Motion balance filtering. *Computer Graphics Forum 19(3)*, 437–446.

VAN DE PANNE, M., FIUME, E., AND VRANESIC, Z. 1992. Control techniques for physically-based animation. In *Proceedings of the Third Eurographics Workshop on Animation and Simulation*.

VAUGHAN, C., DAVIS, B., AND O'CONNOR, J. 1999. *Dynamics of Human Gait (2nd edition)*. Kiboho Publisher.

YAMANE, K., AND NAKAMURA, Y. 2003. Dynamics filter - concept and implementation of on-line motion generator for human figures. *IEEE Transactions on Robotics and Automation 19(3)*, 421–432.

ZHAO, J., AND BADLER, N. 1994. Inverse kinematics positioning using nonlinear programming for highly articulated figures. *ACM Transactions on Graphics 13 (4)* (October), 313–336.

ZORDAN, V., AND HODGINS, J. 2002. Motion capture-driven simulations that hit and react. In *SCA '02: Proceedings of the 2002 ACM SIGGRAPH/Eurographics symposium on Computer animation*, 89–96.

ZORDAN, V., AND VAN DER HORST, C. 2003. Mapping optical motion capture data to skeletal motion using a physical model. In *ACM Siggraph / Eurographics Symposium on Computer Animation*, 245–250.

ZORDAN, V., MAJKOWSKA, A., CHIU, B., AND FAST, M. 2005. Dynamic response for motion capture animation. *ACM Transactions on Graphics 24 (3)* (July), 697–701.
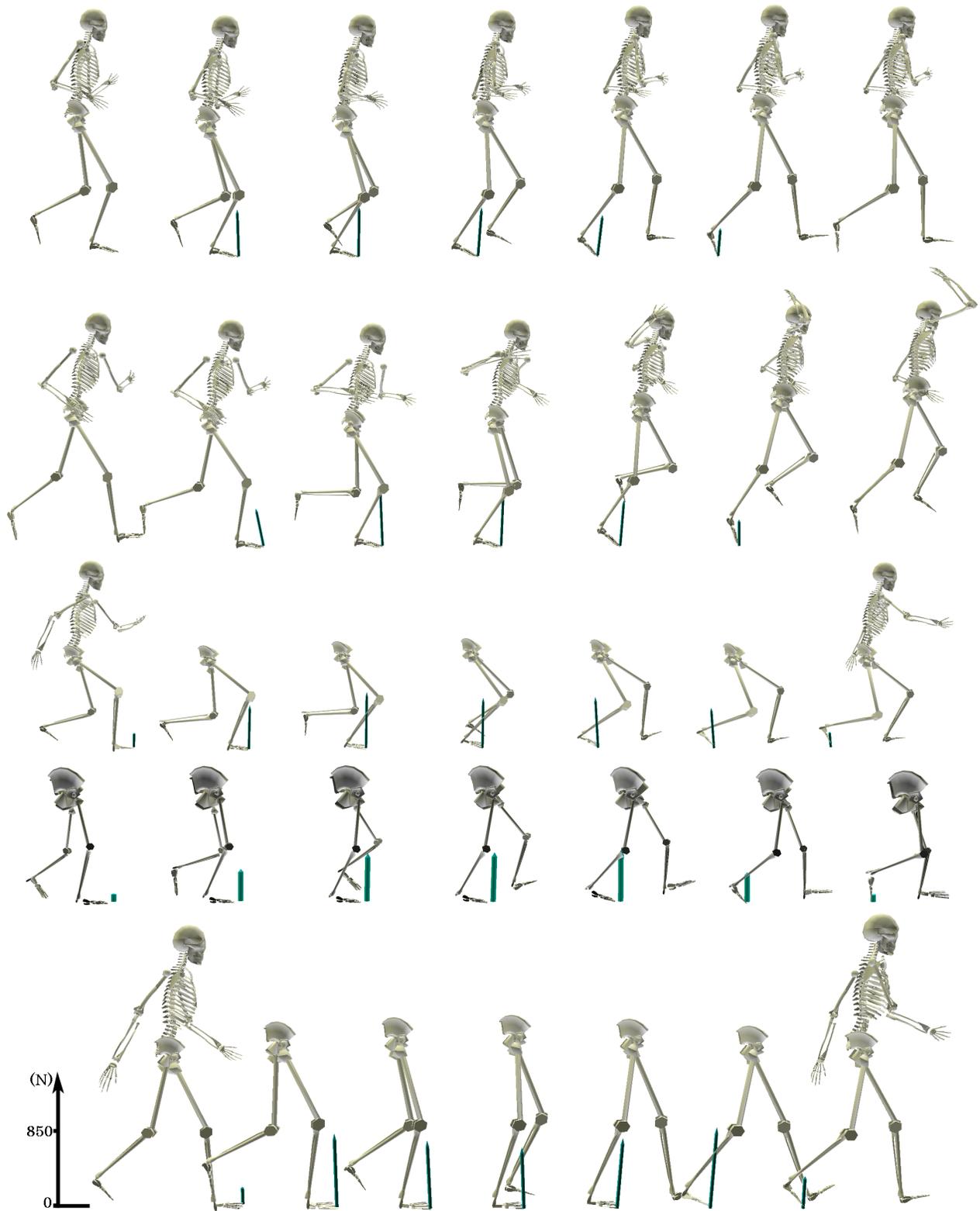
Figure 12: Ground reaction force on the right foot during support phase. First: a running locomotion of a normal adult male. Second: a one-foot jump (handball shooting). Third: a bent walk of a man. Fourth: a walk of a 2 year old child. Fifth: a normal walk of a woman.